Hybrid Approach for Palmprint Recognition Using Compound Features

N.L. Manasa, A. Govardhan, and Ch. Satyanarayana

Jawaharlal Nehru Technological University, Andhra Pradesh, India

Abstract. As patterns in a palmprint have abundance of invariance, the inter-class and intra-class variability of these features makes it difficult for just one set of features to capture this variability. This inspires us to propose a hybrid feature extraction and fusion approach for palmprint recognition based on texture information available in the palm. Scale, shift and rotation (Affine) invariance, good directional sensitivity properties of Dual-tree Complex Wavelets makes it a choice to capture texture features at global level. Local Binary Pattern on the other hand being gray-scale and rotation invariant, captures local fine textures effectively. These local features are sensitive to position and orientation of the palm image. Canonical Correlation Analysis is used to combine the features at the descriptor level which ensures that the information captured from both the features are maximally correlated and eliminate the redundant information giving a more compact representation. Experimental results demonstrate an accuracy of 97.2% at an EER of 3.2% on CASIA palmprint database.

1 Introduction

Human vision system uses both global and local features to recognize the object of interest, and hybrid approaches are thus expected to be promising for palmprint recognition [21]. While ridge like patterns, valleys, minutae points and pores can be extracted only from a high-resolution image, with at least 400 dpi (dots per inch), features like principal lines and wrinkles can be extracted from a low-resolution image, with less than 100 dpi. Though ridge based authentication systems exist for latent palmprint recognition [7], the time consumed in image acquisition and processing restrict them from being used extensively in civil applications.

Creases/Palm lines, the evident structural features on the palm are formed several months after conception. Principal lines which are a result of genetic effects, though are significant, they alone cannot represent the uniqueness of a palmprint as twins and any two people can have similar principal lines as depicted in Fig 2. Palm wrinkle based authentication systems are counter-productive as the constancy of wrinkles can be compromised as they have chances of vanishing/diminishing over time or with extensive physical work with hands. Also few wrinkles are only stable for several months or years after conception. Palm line based approaches [9][10] which rely on derivatives of Gaussian and extraction of

R. Prasath and T. Kathirvalavakumar (Eds.): MIKE 2013, LNAI 8284, pp. 16–27, 2013.

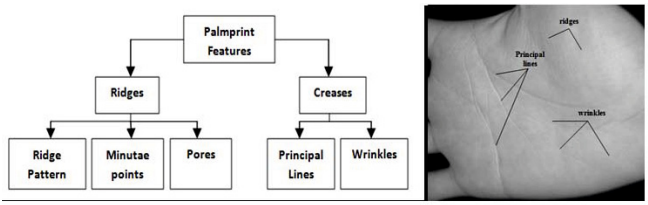

Fig. 1. Different kinds of features on a palmprint

width and location information of palm lines respectively were proposed which suffer from the non-permanence of the chosen features. Successful methods like Palmcode[5], Fusion code[18] and Competitive code[19] which rely on palmlines and their orientations, though attain high accuracy and low error rates, are subject to instability and are not self-sustained for the above reasons. Structural similarities among Palmcodes from palms can be observed from [2].

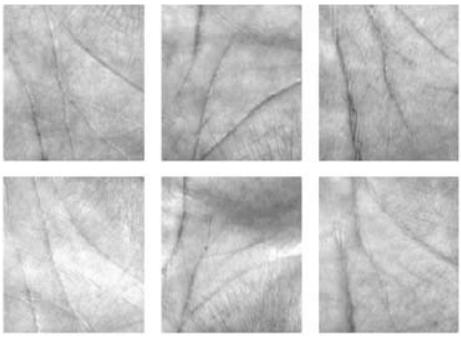

Fig. 2. Images of different individuals with similar principal lines. Courtesy [1].

Along with being permanent, a feature for human authentication should exhibit exclusiveness and idiosyncrasy. It should prove large variance between persons and small variance between samples of the same palm. Another feature that can be extracted from low-resolution palmprint images is Texture. Low-resolution palmprint images can also be considered as texture images. Texture is one of the clearly observable, permanent, distinguishable features on the human palm. This peculiarity inspires us to pursue a reliably working palmprint authentication system based on texture description. Palmprint samples from different individuals having distinctive texture features can be seen from Fig 3.

Texture on the palm can be clearly described by both, features at the local level and at the global level. Global palmprint features possess the following characteristics: (a) insensitive to noise; (b) insensitive to shift changes; (c) easy to compute; and 4) have high convergence within the group and good dispersion between groups [4]. Global features can lower the effect raised by local noises thus supplementing each other. Motivation for the proposed approach is as follows,

1. Although palmprint patterns are diverse among individuals, it is very difficult to distinguish solely based on global texture features as some of these patterns are so similar at a coarse level.
2. Most of the widely popular coding-based methods like palmcode [5] neglect the multiscale characteristic of palm lines [3] and construct authentication systems based on structural similarity.
3. In a peg-free and unconstrained acquisition environment, translation and rotation variations are inevitable. Image description at a local level handles such interferences reasonably [6].

A hand-based hierarchical authentication system [11] was developed to ensure fast matching which uses hand-geometry features at the coarse-level which are unstable in unconstrained environments. [8] demonstrated that the way to improve performance is intra-modal combination of texture-based, line-based and appearance-based features in the palm. They used various score-level and decision-level fusion techniques and claimed the superior performance of product of sum rule which still had higher error rates. [4] designed a hierarchical palmprint recognition approach and thus inferred that local features perform better than hierarchical approach when false acceptance rate is more than 5%.

Hence, all these factors inspired us to propose a hybrid approach which performs a feature-level fusion of local and global texture features of the palm. The above methods fuse the features at the image level where as the proposed method maximizes the correlation between the feature sets at feature level. Although a palmprint authentication system consists of several stages viz., Image Acquisition, Preprocessing/Region-of-interest (ROI) extraction, Feature extraction and Matching, the first two stages are out of the scope of this paper. Image Acquisition can be referred from [12] and ROI extraction proceeds similarly as stated in [1]. Distinctive from the literature, we propose the following hybrid approach to

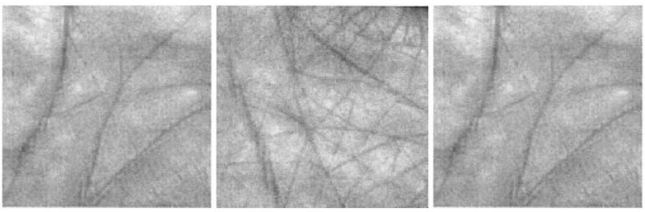

Fig. 3. Samples of different palmprint patterns with distinctive texture features (left) Strong principal lines. (middle) Less wrinkles. (right) Strong wrinkles. Courtesy [1]

overcome the above mentioned challenges and drawbacks. A feature descriptor fusion method based on Canonical Correlation Analysis is used to combine two features, a global feature set and a local feature descriptor: Dual-tree complex wavelets [DTCW][16] and Local Binary Patterns (LBP)[15] respectively. Canonical Correlation Analysis (CCA) is one of the important statistical multi-data processing methods which deals with the mutual relationships between two random vectors. This allows us to capture not only the crease features of the palm

but also captures ridge features, palm-line orientation information and magnitude features as all these can be perceived as local texture [3].

As patterns in the palmprint have abundance of invariance, the inter-class and intra-class variability of these features makes it difficult for just one set of features to capture this variability. The Global features are insensitive to affine transformations, noise, and captures large between-class variance and small within-class variance while Local features capture significant within-class variance. DTCW captures the global information ensuring scale-invariance and shift-invariance which helps in discriminating between locally similar regions. All these properties along with its good directional selectivity in 2D ensure favorable recognition of similar patterns [13]. DTCW features compensate the error in localizing the palm region as they are invariant to the rotation and the inexact localization. The LBP on the other hand captures local fine textures effectively, they are also sensitive to position and orientation of the palm image. It is a powerful texture descriptor that is gray-scale and rotation invariant [14]. A chance of recognition rate being compromised in the case of very large databases is high with different palmprint images having similar global features. Hence it is important to use local texture features in combination with global texture features for accurate recognition.

The proposed method relies on coarse ROI localization and extracts both the feature descriptors. Canonical correlation analysis is used to combine the features at the descriptor level which ensures that the information captured from both the features are maximally correlated and eliminate the redundant information giving a more compact representation.

2 Global and Local Feature Extraction

2.1 Dual-Tree Complex Wavelet Features

Discrete Wavelet Transforms based methods have been successfully applied to a variety of problems like denoising, edge detection, registration, fusion etc., Discrete wavelet transforms have 4 basic problems such as Oscillation, Shift variance, Aliasing and Lack of directionality. By using complex valued basis functions instead of real basis functions these four problems can be minimized. This change is inspired by the Fourier transform basis functions. Complex wavelet transform (CWT) [16] is represented in form of complex valued scaling functions and complex valued wavelet functions.

$$\psi_c(t) = \psi_r(t) + j\psi_i(t) \tag{1}$$

$\psi_r(t)$ are real and even and $j\psi_i(t)$ are imaginary and odd. $\psi_r(t)$ and $\psi_i(t)$ form a Hilbert transform pair (90^o out of phase each others) and $\psi_c(t)$ is the analytics signal. Complex scaling function is also defined in similar ways. Projecting the signal onto $2^{j/2}\psi_c(2^j t - n)$, obtain complex wavelet transforms as follows,

$$d_c(j,n) = d_r(j,n) + jd_i(j,n) \tag{2}$$

In the Complex Wavelet domain, analysis depends on two factors, frequency content (which is controlled by scale factor j) and different time (which is controlled by time shift n).

The dual tree CWT employs two real discrete wavelet transforms (DWT); the first DWT gives the real part of the transform while the second DWT gives the imaginary part. The analysis Filter Bank (FB) used to implement the dual-tree CWT is illustrated in Fig 4.

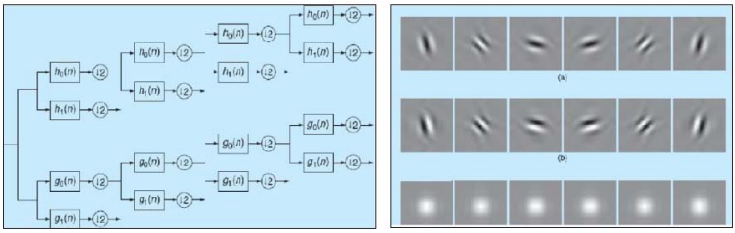

Fig. 4. (left)DTCW filter bank. (right)Typical wavelets associated with the 2-D dual-tree CWT. (a) illustrates the real part of each complex wavelet; (b) illustrates the imaginary part; (c) illustrates the magnitude. Courtesy [16]

To design an overall transform we use two sets of filters. Each set of filter represents real wavelet transform. This overall tranform is approximately analytic. Let $h0(n), h1(n)$ denote the low-pass/high-pass filter pair for the upper FB, and let $g0(n), g1(n)$ denote the low-pass/high-pass filter pair for the lower FB. Denote the two real wavelets affiliated to each of the two real wavelet transforms as $\psi_h(t)$ and $\psi_g(t)$. Filters are designed so that the complex wavelet definition in Equ 1 is approximately estimated. Equivalently, they are designed so that $\psi_g(t)$ is approximately the Hilbert transform of $\psi_h(t)$ [denoted as $\psi_g(t) \approx H\psi_h(t)$]. If the two real DWTs are characterized by the square matrices F_h and F_g, then the dual-tree CWT can be represented by

$$\mathbf{F} = \begin{bmatrix} \mathbf{F}_g \\ \mathbf{F}_h \end{bmatrix} \tag{3}$$

If the vector x represents a real signal, then $w_h = F_h x$ represents the real part and $w_g = F_g x$ represents the imaginary part of the dual-tree CWT. The complex coefficients are given by $w_h + jw_g$.

In dual-tree CWT, consider the 2-D wavelet $\psi(x, y) = \psi(x)\psi(y)$ associated with the row-column implementation of the wavelet transform, where $\psi(x)$ is a complex wavelet given by $\psi(x) = \psi_h(x) + j\psi_g(x)$. Obtain $\psi(x, y)$ for the expression,

$$\begin{aligned} \psi(x,y) &= [\psi_h(x) + j\psi_g(x)][\psi_h(y) + j\psi_g(y)] \\ &= \psi_h(x)\psi_h(y) - \psi_g(x)\psi_g(y) \\ &+ j[\psi_g(x)\psi_y(x) + \psi_h(x)\psi_g(y)] \end{aligned} \tag{4}$$

Take the real part of this complex wavelet, then obtain the sum of two divisible wavelets

$$RealPart\psi(x,y) = \psi_h(x)\psi_h(y) - \psi_g(x)\psi_g(y) \tag{5}$$

We perform a 4-level decomposition and compute the wavelet energy (square sum of wavelet coefficients around 5x5 window) of the real-part at each level and use this as feature vector. These parameters were empirically determined to attain highest accuracies for palmprint recognition experiments presented in this paper.

2.2 Local Binary Pattern Features

LBP captures the local level texture variations. Local binary patterns introduced by Ojala et al. [15] use local texture descriptor. In its simplest form, an LBP description of a pixel is created by thresholding the values of the 3x3 neighborhood of the pixel against the central pixel and explicating the result as a binary number. The Local binary pattern (LBP) operator was originally designed as a texture descriptor. The LBP operator attributes a label to every pixel of an image by thresholding the 3x3 neighborhood of each and every pixel value with the center pixel value and assigns binary value (0,1) based on the following equation,

$$I(x,y) = \begin{cases} 0 & \text{if } N(x,y) < I(x,y) \\ 1 & \text{else} N(x,y) \geq I(x,y) \end{cases}$$

where $I(x,y)$ is the center pixel value and $N(x,y)$ is neighborhood pixel value. After thresholding, central pixel value is represented by a binary number (or decimal number) called label. Histogram of these labels is used as texture descriptor. LBP operator is extended to scale invariance and rotation invariance texture operator for images.

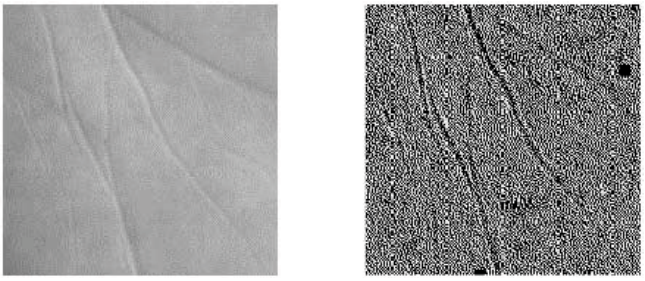

Fig. 5. (left) Extracted 128x128 palm ROI. (right) LBP features on the ROI.

LBP operator deals with textures at different scales using neighborhoods of different sizes. Local neighborhood can be defined using circular neighborhood. Circular neighborhood is a set of evenly spaced sampling points on a circle, whose center is the pixel to be labeled. Radius of circle controls the spatial resolution of operator and number of sampling points controls angular space quantization.

Interpolation is used when a sampling point does not fall in the mediate of a pixel. Notation (P; R) will be used for pixel neighborhoods which contemplates P sampling points on a circle of radius of R.

Fig 5 shows the extracted LBP features of the segmented Region-of-interest on the palm image. To achieve the gray level invariance we subtract the center pixel value with all circular neighborhood pixel values and assume that this difference is independent of center pixel value.

3 Feature Fusion and Matching

Canonical correlation analysis can be defined as the complication of finding two sets of basis vectors, one for $\mathbf{x}$ and one for $\mathbf{y}$, in a way that the correlations between the projections of the variables onto these basis vectors are mutually maximized. Linear combinations $x = \mathbf{x}^T\hat{\mathbf{w}}_x$ and $y = \mathbf{y}^T\hat{\mathbf{w}}_y$ of the two variables is maximized as follows,

$$\rho = \frac{E[xy]}{\sqrt{E[x^2]E[y^2]}} = \frac{E[\hat{\mathbf{w}}_\mathbf{x}^\mathbf{T}\mathbf{x}\mathbf{y}^\mathbf{T}\hat{\mathbf{w}}_\mathbf{y}]}{\sqrt{E[\hat{\mathbf{w}}_\mathbf{x}^\mathbf{T}\mathbf{x}\mathbf{x}^\mathbf{T}\hat{\mathbf{w}}_\mathbf{x}]\mathbf{E}[\hat{\mathbf{w}}_\mathbf{y}^\mathbf{T}\mathbf{y}\mathbf{y}^\mathbf{T}\hat{\mathbf{w}}_\mathbf{y}]}} = \frac{\mathbf{w}_x^T\mathbf{C}_{xy}\mathbf{w}_y}{\sqrt{\mathbf{w}_x^T\mathbf{C}_{xx}\mathbf{w}_x\mathbf{w}_y^T\mathbf{C}_{yy}\mathbf{w}_y}} \tag{6}$$

The maximum of ρ with respect to $\mathbf{w_x}$ and $\mathbf{w_y}$ is the maximum canonical correlation.

$$\begin{cases} E[x_i x_j] = E[\mathbf{w}_{xi}^T\mathbf{x}\mathbf{x}^T\mathbf{w}_{xj}] = \mathbf{w}_{xi}^T\mathbf{C}_{xx}\mathbf{w}_{xj} = 0 \\ E[y_i y_j] = E[\mathbf{w}_{yi}^T\mathbf{y}\mathbf{y}^T\mathbf{w}_{yj}] = \mathbf{w}_{yi}^T\mathbf{C}_{yy}\mathbf{w}_{yj} = 0 \\ E[x_i y_j] = E[\mathbf{w}_{xi}^T\mathbf{x}\mathbf{y}^T\mathbf{w}_{yj}] = \mathbf{w}_{xi}^T\mathbf{C}_{xy}\mathbf{w}_{yj} = 0 \end{cases}$$

The projections onto $\mathbf{w}_x$ and $\mathbf{w}_y$, i.e. x and y, are called canonical variates.

$$a^2 + b^2 = c^2 \tag{7}$$

The covariance matrix between two random variables $\mathbf{x}$ and $\mathbf{y}$ with zero mean is defined as.

$$\mathbf{C} = \begin{bmatrix} \mathbf{C}_{xx} & \mathbf{C}_{xy} \\ \mathbf{C}_{yx} & \mathbf{C}_{yy} \end{bmatrix} = E\left[\begin{pmatrix} \mathbf{x} \\ \mathbf{y} \end{pmatrix} \begin{pmatrix} \mathbf{x} \\ \mathbf{y} \end{pmatrix}^T \right] \tag{8}$$

where $\mathbf{C}$ is a block matrix where $\mathbf{C}_{xx}$ and $\mathbf{C}_{yy}$ are the within-sets covariance matrices of $\mathbf{x}$ and $\mathbf{y}$ respectively and $\mathbf{C}_{xy} = \mathbf{C}_{yx}^T$ is the between-sets covariance matrix. The canonical correlations between $\mathbf{x}$ and $\mathbf{y}$ can be found by solving the eigenvalue equations

$$\begin{cases} \mathbf{C}_{xx}^{-1}\mathbf{C}_{xy}\mathbf{C}_{yy}^{-1}\mathbf{C}_{yx}\hat{\mathbf{w}}_x = \rho^2\hat{\mathbf{w}}_x \\ \mathbf{C}_{yy}^{-1}\mathbf{C}_{yx}\mathbf{C}_{xx}^{-1}\mathbf{C}_{xy}\hat{\mathbf{w}}_y = \rho^2\hat{\mathbf{w}}_y \end{cases} \tag{9}$$

where the eigenvalues ρ^2 are the squared canonical correlations and the eigenvectors $\hat{\mathbf{w}}_x$ and $\hat{\mathbf{w}}_y$ are the normalized canonical correlation basis vectors. The number of non-zero solutions to these equations are limited to the smallest dimensionality of $\mathbf{x}$ and $\mathbf{y}$.

Just one of the eigenvalue equations needs to be solved since the solutions are related by

$$\begin{cases} \mathbf{C}_{xy}\hat{\mathbf{w}}_y = \rho\lambda_x\mathbf{C}_{xx}\hat{\mathbf{w}}_x \\ \mathbf{C}_{yx}\hat{\mathbf{w}}_x = \rho\lambda_y\mathbf{C}_{yy}\hat{\mathbf{w}}_y, \end{cases} \tag{10}$$

where

$$\lambda_x = \lambda_y^{-1} = \sqrt{\frac{\hat{\mathbf{w}}_y^T\mathbf{C}_{yy}\hat{\mathbf{w}}_y}{\hat{\mathbf{w}}_x^T\mathbf{C}_{xx}\hat{\mathbf{w}}_x}}. \tag{11}$$

As discussed below, we apply method proposed by [17] to combine the output of DTCW and LBP and maximize the information present in these two feature vectors.

Let the two feature extractors be trained by L training images. Let $A = [a_1, a_2, ..., a_L]$ and $B = [b_1, b_2, ..., b_L]$ be the corresponding outputs of the two extractors, and n1 and n2 be the dimensions of the two outputs, where $n1, n2 \leq L1$.

The covariance matrices for $\mathbf{A}$ and $\mathbf{B}$ are given as $\mathbf{C}_{aa}$ and $\mathbf{C}_{bb}$ respectively. $\mathbf{C}_{ab}$ is the between-set covariance matrix. $\hat{\mathbf{w}}_x$ and $\hat{\mathbf{w}}_y$ are canonical basis vectors of feature vectors $\mathbf{A}$ and $\mathbf{B}$. a_i and b_i are two feature vectors of image i. Fusion of these two feature vectors is defined as,

$$\mathbf{F}_i = \begin{bmatrix} \hat{\mathbf{w}}_x^T a_i \\ \hat{\mathbf{w}}_y^T b_i \end{bmatrix} = \begin{bmatrix} \hat{\mathbf{w}}_x & 0 \\ 0 & \hat{\mathbf{w}}_y \end{bmatrix}^T \begin{bmatrix} a_i \\ b_i \end{bmatrix} \tag{12}$$

For the matching purpose we use cosine similarity measure. Cosine similarity measure is defined as cosine angle between test image fused feature vector and training images fused feature vector,

$$\arg max_{j\in[1,2\cdots L]} \left(\frac{\mathbf{F}_i^T\mathbf{F}_j}{\|\mathbf{F}_i\|\cdot\|\mathbf{F}_j\|} \right) \tag{13}$$

The maximum value according to Equ(13) is estimated as an authenticated palmprint match.

4 Experiments and Results

We test our algorithm on publicly available CASIA database [12], which contains 5502 palm images of 312 subjects from both left and right palms. There are no pegs to restrict postures and positions of palms hence leading to several palm localization issues. To the best of our knowledge this database is the largest publicly available database in terms of number of subjects [3]. 80% of the images are used as training samples and remaining are used for testing purpose. We resize the images to 128x128.

In first of our experiments, we check for recognition accuracy using DTCW and LBP feature separately. Highest recognition rate of Dual-tree and LBP are 90.8% and 92.6% with 128 and 150 lengths feature vector respectively. Refer Fig 6 which plots the recognition rate vs feature vector length.

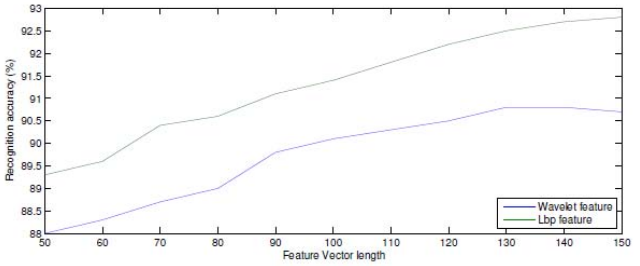

Fig. 6. Recognition performance of individual methods, DTCW and LBP

We perform the second experiment to illustrate the superior performance of CCA based fusion framework over two other widely used fusion methods: Sum rule and Max rule [6]. Fig 7 shows recognition accuracy of three fusion methods used at variable feature vector length. Fusion of these two features improves the recognition rate. Highest recognition rate attained from fusion using Sum rule, Max rule and CCA reached 93.8%, 95.2% and 97.2% respectively with feature vector length 200.

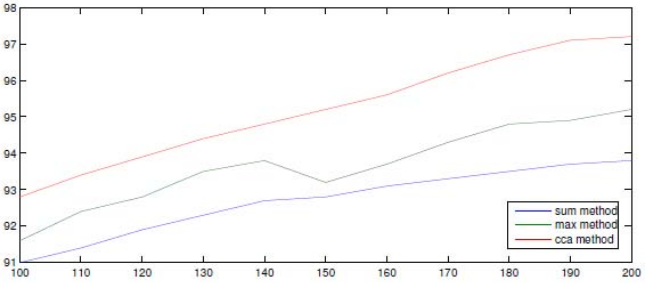

Fig. 7. Accuracy of different fusion methods at variable feature vector length

Hence we infer that local features perform better than global features for palmprint recognition and fusion using Max rule considerably improves the recognition accuracy in comparison with Sum rule. We also establish that Canonical Correlation based fusion outperforms other methods with an EER of 3.2%. See Fig 8.

In [13] DTCW with SVM was used for palmprint recognition on PolyU database which attains an accuracy of 97%. Significant performance of our approach can be noted by comparing the complicacy of CASIA database to PolyU database. As stated in [3 - Table 1 and Table 5], error rates obtained on CASIA are much higher than those obtained on PolyU database. The assumed reasons for this being,

1. The quality of the palm images in CASIA was lesser than those in PolyU as CASIA images were captured using web camera.

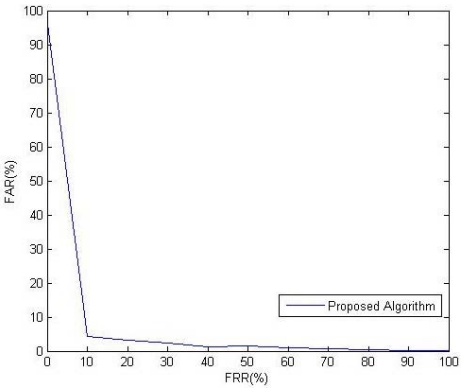

Fig. 8. Receiver Operating Characteristics curve for the proposed method on CASIA palmprint database

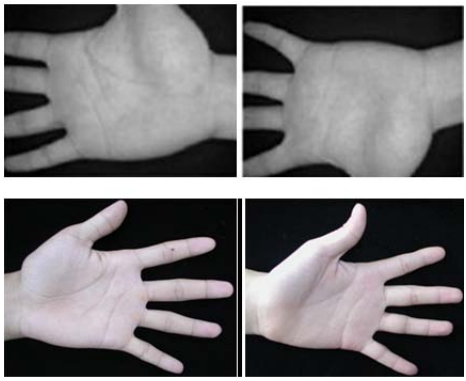

Fig. 9. Palmprint image samples from (top)CASIA palmprint database (bottom)UST hand Image database

2. There are no pegs to restrict postures and positions of palms during data acquisition hence leading to several localization issues like translation, rotation, scaling, varied illumination because of the degrees of freedom.
3. As CASIA is a large database in terms of number of subjects (no. of palms) than PolyU which might degrade the recognition accuracy.

In [14] palmprint identification using Local Binary Pattern and Adaboost was proposed and an Equal Error Rate (EER) of 2% was reported which is much lesser than our EER of 3.2%. Again to justify this, we compare CASIA database to UST hand Image database [20] on which results in [14] were shown. While palmprint images in UST database had a resolution of 24 bits, CASIA palmprints are 8-bit gray-level images. This difference is evident from Fig 8. One more reason might be the selection of discriminative local binary patterns using Adaboost.

In [6], a similar framework based on local and global feature fusion was proposed. Good performance of 97.8% was reported with Sum-rule. We attribute the gain in accuracy on the complicacy of the database used. The internal/private database used in this paper had (a) scanner-based image acquisition system, (b) small in size with 1000 palmprint images from 100 subjects.

5 Conclusion

In this paper, a hybrid feature extraction and fusion framework based on texture information for palmprint recognition is proposed. DTCW captures the global information ensuring scale-invariance and shift-invariance which helps in discriminating between locally similar regions. LBP on the other hand being gray-scale and rotation invariant, captures local fine textures effectively. Improvement in performance is reported by combining these features using three different fusion rules, of which Canonical Correlation based fusion approach is most promising. Through the fusion framework, more than 5% performance gain over single extraction method is reported. In comparison with three other methods [13] [14] [6] which proceed on the similar lines, advantages of our approach are established by supporting reasoning/inferences.

Acknowledgments. Portions of the research in this paper use the CASIA Palmprint Database collected by the Chinese Academy of Sciences Institute of Automation (CASIA). Authors would like to appreciate the efforts in constructing the database.

References

1. Zhang, D., Kong, W.K., You, J., Wong, M.: Online palmprint identification. IEEE Trans. Pattern Anal. Mach. Intell. 25(9), 1041–1050 (2003)
2. Kong, A.W.-K., Zhang, D.: Feature-Level Fusion for Effective Palmprint Authentication. In: Zhang, D., Jain, A.K. (eds.) ICBA 2004. LNCS, vol. 3072, pp. 761–767. Springer, Heidelberg (2004)
3. Zuo, W., Lin, Z., Guo, Z., Zhang, D.: The multiscale competitive code via sparse representation for palmprint verification. In: Proc. of CVPR, pp. 2265–2272 (2010)
4. You, et al: On hierarchical palmprint coding with multiple features for personal identification in large databases. IEEE Trans. Circuits Syst. Video Tech. (2004)
5. Kong, W., Zhang, D., Li, W.: Palmprint feature extraction using 2-d gabor filters. Pattern Recog. 36(10), 2339–2347 (2003)
6. Pan, et al.: Palmprint recognition using fusion of local and global features. In: Proc. of the Int. Symposium on Intelligent Signal Processing and Communication Systems, pp. 642–645 (2007)
7. Jain, A., Feng, J.: Latent palmprint matching. IEEE Trans. Pattern Anal. Mach. Intell. 31(5), 1032–1047 (2009)
8. Kumar, A., Zhang, D.: Personal authentication using multiple palmprint representation. Pattern Recognition 38, 1695–1704 (2005)
9. Wu, X., Zhang, D., And Wang, K.: Palm line extraction and matching for personal authentication. IEEE Trans. Syst. Man Cybern. Part A 36(5), 978–987 (2006b)

10. Liu, L., Zhang, D., You, J.: Detecting wide lines using isotropic nonlinear filtering. IEEE Trans. Image Process. 16(6), 1584–1595 (2007)
11. Han, C.-C.: A hand-based personal authentication using a coarse-to-fine strategy. Image and Vision Computing 22, 909–918 (2004)
12. CASIA Palmprint database, http://www.idealtest.org/dbDetailForUser.do?id=5
13. Chen, G.Y., Xie, W.F.: Pattern recognition with SVM and dual-tree complex. Image and Vision Computing 25(6), 960–966 (2007)
14. Wang, et al: Palmprint identification using boosting local binary pattern. In: Proceedings of ICPR, pp. 503–506 (2006)
15. Ojala, et al: Multiresolution gray-scale and rotation invariant texture classification with Local Binary Patterns. IEEE Transactions on PAMI 24(7), 971–987 (2002)
16. Selesnick, et al.: The dual-tree complex wavelet transform. IEEE Signal Processing Magazine 22(2), 123–151 (2005)
17. Sun, Q.-S., et al.: A theorem on the generalized canonical projective vectors. Pattern Recognition 38, 449–452 (2005)
18. Kong, A., Zhang, D., Kamel, M.: Palmprint identification using feature-level fusion. Pattern Recog. 39(3), 478–487 (2006a)
19. Kong, A., Zhang, D.: Competitive coding scheme for palmprint verification. In: Proceedings of the 17th International Conference on Pattern Recognition, pp. 520–523 (2004)
20. UST Hand Image database, http://www4.comp.polyu.edu.hk/~csajaykr/Database/palm/2dhand.html
21. Zhang, et al.: A Comparative Study of Palmprint Recognition Algorithms. ACM Computing Surveys 44(1) (2012)